Inorganic Chemistry
Article

Inorg. Chem. **2010**, *49*, 3271–3277 **3271**
DOI: 10.1021/ic902255j

Metal Dilution Effects on Entropy and Light-Induced Valence Tautomeric Interconversion in a 1:1 Cobalt−Dioxolene Complex

A. Dei,* G. Poneti, and L. Sorace

Laboratory of Molecular Magnetism (LAMM), Department of Chemistry, Ugo Schiff and INSTM Research Unit, University of Florence, Via della Lastruccia, 3-13, 50019 Sesto Fiorentino, Florence, Italy

Received November 14, 2009

The entropy and the light-induced valence tautomeric interconversions of solid solutions of the $[Co(Me_2tpa)(diox)](PF_6)\cdot C_6H_5CH_3$ complex [Me_2tpa = bis(6-methyl-(2-pyridylmethyl))(2-pyridylmethyl)amine and diox = catecholato (DBCat) or semiquinonato (DBSQ) forms of 3,5-ditert-butylquinone] in the electronically innocent $[Zn(Me_2tpa)(DBSQ)](PF_6)\cdot C_6H_5CH_3$ host, in four different molar ratios, have been investigated. It has been found that the entropy driven transition is strongly affected by the Co:Zn molar ratio, whereas the relaxation rates of the optically induced high-spin Co^{II}−DBSQ metastable state at cryogenic temperatures are nearly independent of the degree of solid dilution. These results are discussed in the framework of the Jortner theory for adiabatic radiationless multiphonon relaxation processes. It is suggested that the optical bistability in these systems is related to the single molecule properties rather than to the cooperative effects active in the lattice.

Introduction

Molecular systems undergoing redox isomerism (valence tautomerism, VT) following external stimuli have attracted considerable attention.[1−3] This phenomenon has been detected in several classes of materials, such as Mn−, Co−, and Cu−dioxolene complexes,[4−8] polycyanometallato derivatives,[9−12] and cobalt ferrite nanoparticles.[13] Among metal−dioxolene complexes, the cobalt derivatives have been the most investigated systems up to now.[14−18] In these compounds, redox isomerism involves an intramolecular electron transfer (ET) between the coordinated ligand and the metal ion, which yields an interconversion between low-spin (ls)-Co^{III}−catecholate and high-spin (hs)-Co^{II}−semiquinonate charge distributions. Temperature,[14−20] pressure,[21−23] light irradiation,[24−30] and magnetic fields[31] have been found to be effective in inducing the ET process. Since

*Corresponding author. Telephone: +39 055 4573280. Fax: +39 055 4573372. E-mail: andrea.dei@unifi.it.

(1) Sato, O.; Tao, J.; Zhang, Y.-Z. *Angew. Chem., Int. Ed. Engl.* **2007**, *46*, 2152–2187.
(2) Sato, O. *J. Photochem. Photobiol.* **2004**, *5*, 203–223.
(3) *Magnetism: Molecule to Materials*; Miller, J. S., Drillon, M., Eds.; Wiley-VCH: Weinheim, Germany, 2001−2005.
(4) Hendrickson, D. N.; Pierpont, C. G. *Top. Curr. Chem.* **2004**, *234*, 63–95.
(5) Pierpont, C. G. *Coord. Chem. Rev.* **2001**, *216−217*, 99–125.
(6) Shultz, D. A. In *Magnetism: Molecules to Materials*, Vol. *2*; Miller J. S., Drillon M., Eds.; Wiley-VCH: Weinheim, Germany, 2001, pp. 281−306
(7) Gütlich, P.; Dei, A. *Angew. Chem., Int. Ed. Engl.* **1997**, *36*, 2734–2736.
(8) Evangelio, E.; Ruiz-Molina, D. *Eur. J. Inorg. Chem.* **2005**, 2957–2971.
(9) Sato, O.; Iyoda, T.; Fujishima, A.; Hashimoto, K. *Science* **1996**, *272*, 704–705.
(10) Verdaguer, M. *Science* **1996**, *272*, 698–699.
(11) Bleuzen, A.; Lomenech, C.; Escax, V.; Villain, F.; Varret, F.; Cartier dit Moulin, C.; Verdaguer, M. *J. Am. Chem. Soc.* **2000**, *122*, 6648.
(12) Dei, A. *Angew. Chem. Int. Ed.* **2005**, *44*, 1160–1163.
(13) Giri, A. K.; Kirkpatrick, E. M.; Moongkhamklang, P.; Majetic, S. A.; Harris, V. G. *Appl. Phys. Lett.* **2002**, *80*, 2341–2343.
(14) Buchanan, R. M.; Pierpont, C. G. *J. Am. Chem. Soc.* **1980**, *102*, 4951–4957.
(15) Adams, D. M.; Dei, A.; Rheingold, A. L.; Hendrickson, D. N. *J. Am. Chem. Soc.* **1993**, *115*, 8221–8229.
(16) Jung, O.-S.; Jo, D. H.; Li, Y.-A.; Conklin, B. J.; Pierpont, C. G. *Inorg. Chem.* **1997**, *36*, 19–24.
(17) Dei, A.; Gatteschi, D.; Sangregorio, C.; Sorace, L. *Acc. Chem. Res.* **2004**, *37*, 827.
(18) Sato, O.; Cui, A.; Matsuda, R.; Tao, J.; Hayami, S. *Acc. Chem. Res.* **2007**, *40*, 361–369.
(19) Jung, O.-S.; Pierpont, C. G. *Inorg. Chem.* **1994**, *33*, 2227–2235.
(20) Dei, A.; Feis, A.; Poneti, G.; Sorace, L. *Inorg. Chim. Acta* **2008**, *361*, 3842–3846.
(21) Roux, C.; Adams, D. M.; Itiè, J. P.; Polian, A.; Hendrickson, D. N.; Verdaguer, M. *Inorg. Chem.* **1996**, *35*, 2846–2852.
(22) Caneschi, A.; Dei, A.; Fabrizi de Biani, F.; Gütlich, P.; Ksenofontov, V.; Levchenko, G.; Hoefer, A.; Renz, F. *Chem.—Eur. J.* **2001**, *7*, 3924–3930.
(23) Li, B.; Tao, J.; Sun, H.; Sato, O.; Huang, R.-B.; Zheng, L.-S. *Chem. Commun.* **2008**, 2269–2271.
(24) Sato, O.; Hayami, S.; Gu, Z.-Z.; Seki, K.; Nakjima, R.; Fujishima, A. *Chem. Lett.* **2001**, 874–875.
(25) Sato, O.; Hayami, S.; Gu, Z.-Z.; Takahshi, K.; Nakjima, R.; Fujishima, A. *Chem. Phys. Lett.* **2002**, *355*, 169–174.
(26) Neuwahl, F.; Righini, R.; Dei, A. *Chem. Phys. Lett.* **2002**, *352*, 408–414.
(27) Carbonera, C.; Dei, A.; Létard, J. F.; Sangregorio, C.; Sorace, L. *Angew. Chem. Int. Ed.* **2004**, *43*, 3136–3138.
(28) Beni, A.; Carbonera, C.; Dei, A.; Létard, J. F; Righini, R.; Sangregorio, C.; Sorace, L. *J. Braz. Chem. Soc.* **2006**, *17*, 1522–1533.
(29) Beni, A.; Dei, A.; Rizzitano, M.; Sorace, L. *Chem. Commun.* **2007**, 2160–2162.
(30) Beni, A.; Dei, A.; Shultz, D. A.; Sorace, L. *Chem. Phys. Lett.* **2006**, *428*, 400–404.
(31) Markevtsev, I. N.; Monakhov, M. P.; Platonov, V. V.; Mischenko, A. S.; Zvezdin, A. K.; Bubnov, M. P.; Abakumov, G. A.; Cherkasov, V. K. *J. Magn. Magn. Mater.* **2006**, *300*, 407–410.

Published on Web 03/02/2010

this interconversion is associated with large differences in colors and in magnetic properties, these systems are particularly attractive both as constitutive elements of molecule-based devices and as testing grounds of the factors affecting the ET processes.

The possible use of such systems for applicative purposes has been associated in the past to the peculiarity of existing, under the same thermodynamic conditions, in at least two states, featuring different physical or chemical properties.[32−37] This behavior, referred to as bistability, requires an existence of at least two degenerate minima of the free energy of the system under the same conditions of the external parameters (T, P, H, etc.) and a large free energy barrier between the two minima. However, a more appropriate approach to this problem should consider that, for any technological application of these systems, what is actually required is the persistence of the same molecular system in different states for the time required by the technological application. In this sense, the existence of a thermodynamic bistability is a sufficient but not necessary condition. It is only necessary that, in addition to the thermodynamic stable species, the system can exist in a metastable state characterized by an appropriate kinetic stability.

The differences between the two approaches are clearly reflected in the different research lines developed in this field. A first one is focused to obtain systems with T_c (the temperature value at which thermodynamic bistability occurs) close to room temperature and characterized by large thermal hysteresis. The second perspective has been aimed to properly perturb the system to stimulate the conversion between two nondegenerate states. Once the metastable state is populated, the investigation is focused to understand and to control the factors affecting the kinetic of its decay to the thermodynamically stable one. The obvious question is: *are the two approaches providing related answers from the probed physical system?* The work developed up to now, in the strictly connected topic of spin crossover complexes (SC), suggests that the answer to this question should be positive.[38−42]

For these systems, large hysteresis loops were observed on increasing cooperative effects in the lattice, e.g., by building polymeric networks made up by interconverting centers. The significant increase in metal-donor bond lengths associated to the ls/hs interconversion results in a relevant lattice expansion. It was, therefore, suggested that cooperativity arises from both elastic energy and vibrational entropy changes due to anharmonicity of vibrations, both phenomena being a consequence of the expansion of the lattice. While several experiments supported the validity of this approach for the control of cooperativity of thermal interconversions, factors determining the absolute values of thermal transition temperature T_c are far from being quantitatively elucidated.

Also the kinetics of the decay of the metastable state populated at low temperature after an external perturbation (usually optical irradiation) has been interpreted as being controlled by elastic interactions experienced by the interconverting centers in the lattice.[40−42] In particular, on the basis of the analysis of several SC complexes in differently diluted materials, Hauser proposed that the lifetime of the metastable species in the low-temperature region is inversely proportional to the thermal spin-transition temperature T_c. This relationship is known as the inverse energy gap law, since a long lifetime is related to a small difference of the free energy of the two interconverting species.[42] The intrinsic meaning of the law is that the thermal, entropy driven, spin transition is controlled by the same factors which determine the decay kinetics of the optically induced metastable species.

With the aim of defining a standard and simple procedure allowing a rapid comparison of the light-induced properties of different materials and of identifying a parameter characterizing the decay of the photoinduced state, the concept of T_{LIESST} was subsequently developed.[43−47] This is defined as the limit temperature above which the photoexcited stationary state completely relaxes to the ground one by warming the material at a rate of 0.3 K min^{-1}, after having switched off the excitation source at 10 K.[47] In this framework, Létard and co-workers carried out a systematic investigation aimed at establishing a linear correlation between the critical temperature T_c and T_{LIESST}. Unfortunately the results recently reported by the same authors on a series of solid solutions of a spin crossover iron(II) complex in diamagnetic zinc analogues seem to contradict the expected paradigm.[48,49] Indeed, while the T_c values followed the thermodynamic general expectation, T_{LIESST} values were found to be independent of the concentration of the paramagnetic iron(II) complex in the diamagnetic lattice.

Similar considerations are believed to hold for complexes undergoing redox isomerism interconversions, like cobalt−dioxolene complexes as well, since also these transitions are associated with lattice expansions due to the difference in metal-donor bond lengths of the two redox isomers, as first stressed and discussed by Hendrickson.[50] Indeed, the results some of us obtained by using polymeric networks of interconverting moieties support the extension of the same strategies adopted for spin crossover derivatives to VT interconversions for obtaining complexes showing thermal hysteresis.[30,51]

The situation is, however, less clear for the correlation between the T_c of redox isomeric interconversions and the

(32) Feringa, B. L. *Molecular Switches*, Wiley-VCH: Weinheim, Germany, 2001.
(33) de Silva, A. P.; McClenaghan, N. D. *Chem.—Eur. J.* **2004**, *10*, 574.
(34) Kahn, O.; Launay, J. P. *Chemtronics* **1988**, *3*, 140–151.
(35) Aviram, A. *Int. J. Quantum Chem.* **1992**, *42*, 1615–1624.
(36) Kahn, O.; Kröber, J.; Jay, C. *Adv. Mater.* **1992**, *4*, 718–728.
(37) Sessoli, R.; Gatteschi, D.; Caneschi, A.; Novak, M. A. *Nature* **1993**, *365*, 141–143.
(38) Gütlich, P.; Hauser, A.; Spiering, H. *Angew. Chem., Int. Ed. Engl.* **1994**, *33*, 2024–2054.
(39) Gütlich, P.; Garcia, Y.; Woike, T. *Coord. Chem. Rev.* **2001**, *219−221*, 839–879.
(40) Gütlich, P.; Garcia, Y.; Goodwin, H. A. *Chem. Soc. Rev.* **2000**, *29*, 419.
(41) Hauser, A. *Top. Curr. Chem.* **2004**, *234*, 155–198.
(42) Hauser, A.; Enachescu, C.; Daku, M. L.; Vargas, A.; Amstutz, N. *Coord. Chem. Rev.* **2006**, *250*, 1642–1652.
(43) Létard, J.-F.; Guionneau, P.; Rabardel, L.; Howard, J. A. K.; Goeta, A. E.; Chasseau, D.; Kahn, O. *Inorg. Chem.* **1998**, *37*, 4432–4441.
(44) Létard, J.-F.; Capes, L.; Chastanet, G.; Moliner, N.; Létard, S.; Real, J.-A.; Kahn, O. *Chem. Phys. Lett.* **1999**, *313*, 115–120.
(45) Marcén, S.; Lecren, L.; Goodwin, H. A.; Létard, J.-F. *Chem. Phys. Lett.* **2002**, *358*, 87–95.
(46) Létard, J.-F.; Guionneau, P.; Nguyen, O.; Costa, J. S.; Marcén, S.; Chastanet, G.; Marchivie, M.; Goux-Capes, L. *Chem.—Eur. J.* **2005**, *11*, 4582–4589.
(47) Létard, J.-F. *J. Mater. Chem.* **2006**, *16*, 2550–2559.
(48) Baldé, C.; Desplanches, C.; Wattiaux, A.; Guionneau, P.; Gütlich, P.; Lètard, J.-F. *Dalton Trans.* **2008**, 2702–2707.
(49) Baldé, C.; Desplanches, C.; Gütlich, P.; Freysz, E.; Lètard, J.-F. *Inorg. Chim. Acta* **2008**, *361*, 3529–3533.
(50) Adams, D. M.; Hendrickson, D. N. *J. Am. Chem. Soc.* **1996**, *118*, 11515.
(51) Bodnar, S. H.; Caneschi, A.; Dei, A.; Shultz, D. A.; Sorace, L. *Chem. Commun.* **2001**, 2150.

lifetime of the photoinduced metastable state. Indeed, the investigation of a family of 1:1 cobalt−dioxolene complexes of the general formula $[Co^{III}(Me_ntpa)(DBCat)]PF_6$ [Me_ntpa = *n*(6-methyl-(2-pyridylmethyl)) (3-*n*)(2-pyridylmethyl)amine and DBCat = 3,5-ditert-butylcatecholato)] showed that the lifetimes at cryogenic temperatures of the optically induced Co^{II}−semiquinonato form did not follow the regular trend expected from electrochemical data in solution.[52] It was suggested the onset of crystal-packing effects is a crucial factor in determining the thermal dependence of the VT transitions, while smaller consequences are expected on the relaxation rates of the metastable state. Such a conclusion has been strengthened looking at the static and dynamic features of different solvates of $[Co(Me_2tpa)(DBCat)]PF_6$ (**1**).[53] It was indeed observed that T_c shifts of 200 K, changing the crystallization solvent from ethanol to toluene, while comparable relaxation times of the photoinduced hs-Co^{II}−SQ phase have been found at 9 K. In much the same results line, $[Co(Metpa)(DBCat)]PF_6$[52] revealed a longer relaxation time along with a higher T_c with respect to **1,** in open contrast with the expectations. In a similar way, the VT process generally occurs in solution and in solid state at very different temperatures. This implies that the limited degree of our knowledge does not allow a prediction of the ratio between the enthalpy and entropy changes involved in the interconversions.

Since the inverse energy gap law finds its roots in the fundamentals of quantum mechanics, its validity cannot be challenged. However, we thought reasonable to believe that its apparent failure in rationalizing the observed experimental results can be explained, taking into account different lattice interactions. For this reason, we decided to exploit the dilution technique also for cobalt−dioxolene complexes. In this contribution, we report the effect of intermolecular elastic interactions on the conversion properties of the toluene solvate of **1** by diluting it in $[Zn(Me_2tpa)(DBSQ)]PF_6 \cdot C_6H_5CH_3$. This choice was due to the fact that **1** can be nearly quantitatively optically converted to the metastable hs-Co^{II}−DBSQ species at cryogenic temperatures,[53] and the nature of the species involved in the entropy and optically driven valence tautomeric interconversion has been recently supported by X-rays absorption spectroscopy.[54]

Experimental Section

Synthesis. Compound **1** as well as the Zn analogue were synthesized according to the previously reported procedure.[52] Solid solutions of **1** in the Zn host have been obtained by recrystallization from toluene of stoichiometric amounts of the complexes.

Crystallographic Analysis. The structure determination of $[Zn(Me_2tpa)(DBSQ)]PF_6 \cdot C_6H_5CH_3$ was carried out at 120(2) K using an Xcalibur3 (Oxford Diffraction) diffractometer, equipped with a Mo K_α radiation and an Oxford Cryosystems 600 nitrogen flow cryostat. The structure was solved by direct methods using the SIR92 program.[55] Full-matrix least-squares refinement on F_o^2 was performed using the SHELXL-97 program[56] implemented in the WINGX suite.[57] All nonhydrogen atoms were refined anisotropically, with the exception of few disordered moieties. Hydrogen atoms were treated as riding contributors with isotropic displacement parameters. The Cambridge Crystallographic Data Centre (CCDC), via www.ccdc.cam.ac.uk/data_request/cif, contains the supplementary crystallographic data for this paper, CCDC-753733. The data is also supplied in the Supporting Information.

The XRD pattern of 50% doped was recorded on a Bruker D8 Advance diffractometer equipped with Cu K_α radiation and operated in a $\theta-2\theta$ Bragg−Brentano geometry at 40 kV and 40 mA on a microcrystalline powder sample.

Magnetic Measurements. Magnetometric analysis in the function of temperature and light irradiation has been achieved working with a Cryogenic S600 SQUID and a Quantum Design MPMS magnetometers in 1 T applied static field in the 2.5−300 K range. For photomagnetic measurements, the sample (approximately 0.5 mg, the actual Co content being evaluated by scaling the magnetic moment with one of a polycrystalline heavier sample) was mixed with KBr powder and pressed into a pellet to ease light penetration in the whole material. Light irradiation experiments have been performed with a 904 nm CW laser diode coupled with an optic fiber inserted in the sample space through a hollow sample rod and collimated on the sample by means of an aspheric lens, yielding a radiant power on the sample of about 5 mW/cm^2. The reversibility of the process has been checked for all the presented samples. Magnetic moments are corrected for the diamagnetic contribution of the KBr and the sample holder as well as with Pascal constants. T_{LIESST} was measured by monitoring the temperature above which the photoinduced magnetization of the cobalt(II)−semiquinonato metastable phase is erased by warming the material at a rate of 0.3 K min^{-1}, starting from 10 K after having switched off the pumping laser source at the photostationary limit of the compounds. Because of sensitivity reasons, it was not possible to measure the T_{LIESST} value for the photoinduced metastable state of the 0.05 Co molar ratio sample.

Results and Discussion

Synthesis and Crystal Structure. Our approach to the characterization of the dependence of the lifetimes of the photoinduced metastable state of **1** on elastic interactions relies upon the "mixed crystal" technique, in which the complex is dissolved in an inert host crystalline matrix. The chosen crystal host is the $[Zn(Me_2tpa)(DBSQ)]PF_6 \cdot C_6H_5CH_3$ complex because of the ionic radius of Zn^{II}, which is similar to that of the hs-Co^{II} species. Four different solid solutions of formula $[Co_xZn_{(1-x)}(Me_2tpa)(DBSQ)]PF_6 \cdot C_6H_5CH_3$ (x = 0.05, 0.15, 0.25, and 0.50) were prepared to investigate the role of the elastic interactions in the entropy and optically driven valence tautomeric interconversion of **1**. The actual Co molar ratio for each dilution has been assessed by magnetometric means, comparing the high-temperature magnetization with those of the experimental ones of the pure compound **1** and the corresponding pure Zn derivative.

The structure of the pure Zn derivative obtained by single-crystal diffractometry is reported in Figure 1 (left): the asymmetric unit is composed of two molecular units,

(52) Beni, A.; Dei, A.; Laschi, S.; Rizzitano, M.; Sorace, L. *Chem.—Eur. J.* **2008**, *14*, 1804–1813.
(53) Dapporto, P.; Dei, A.; Poneti, G.; Sorace, L. *Chem.—Eur. J.* **2008**, *14*, 10915–10917.
(54) (a) Poneti, G.; Mannini, M.; Sorace, L.; Sainctavit, Ph.; Arrio, M.-A.; Rogalev, A.; Wilhelm, F.; Dei, A. *ChemPhysChem* **2009**, *10*, 2090–2095. (b) Poneti, G.; Mannini, M.; Sorace, L.; Sainctavit, Ph.; Arrio, M.-A.; Otero, E.; Criginski Cezar, J.; Dei, A. *Angew. Chem. Int. Ed.* doi:10.1002/anie.200906895
(55) Altomare, A.; Cascarano, G.; Giacovazzo, C.; Gagliardi, A. *J. Appl. Crystallogr.* **1993**, *26*, 343–350.
(56) Sheldrick, G. M. *SHELX97, Programs for Crystal Structure Analysis (Release 97−2)*, University of Göttingen, Göttingen, Germany, 1997.
(57) Farrugia, L. J. *J. Appl. Crystallogr.* **1999**, *32*, 837–838.

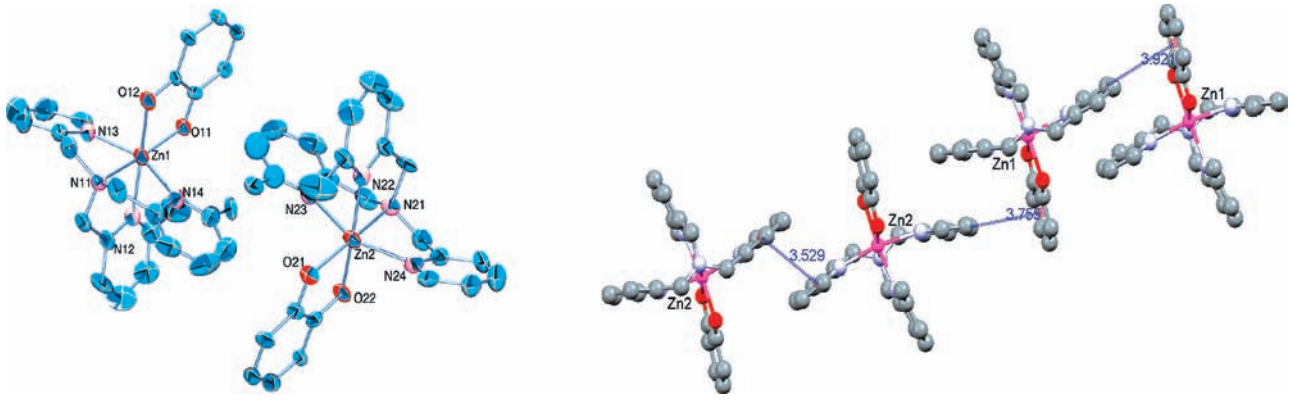

Figure 1. Left: View of the two molecules in the crystallographic-independent cationic moiety of $[Zn(Me_2tpa)(DBSQ)]PF_6 \cdot C_6H_5CH_3$. For clarity sake, the hydrogen atoms and the tert-butyl groups are not shown. Right: Pattern of the C−H···π and π−π intermolecular interactions among adjacent molecules. View along c*.

as already observed for **1**.[53] Each moiety contains a PF_6 anion, a toluene solvent molecule, and a $Zn(Me_2tpa)$-DBSQ monocation. In each of these molecules, the Zn^{II} ion is in a six-coordinate, distorted octahedral coordination with two oxygen- and four nitrogen-donor atoms. The tripodal ligand Me_2tpa adopts a folded conformation around the metal ion, with DBSQ acting as a bidentate ligand. This leads to Zn−N bond lengths in the range 2.156(7)−2.309(9) and 2.138(8)−2.281(9) Å for the two units, while two types of Zn−O distance are observed 2.004(6)−2.016(6) and 2.102(6)−2.136(6) Å. For both the units, the relevant bond lengths in the dioxolene units are in the expected range for the semiquinonato oxidation state,[58] with C−O ranging from 1.270(11) to 1.289(10) and with C1−C2 being 1.454(12) and 1.473(12) Å for each moiety.

The analysis of the crystal packing and the intermolecular contacts also revealed some interesting features. The two molecules constituting the asymmetric unit are interacting through a couple of C−H···π interactions between a semiquinonato ligand on one molecule and an orthogonal pyridine on the adjacent one, with C_{py}−$SQ_{centroid}$ distance of 3.7−4.0 Å. Even more relevant is the stacking interaction between the molecule containing the Zn^{II} center and the adjacent one, which is reported by symmetry. In this case a π−π interaction between pyridine rings, with a distance of 3.5 Å between the respective centroids, is active. The combination of these different interacting paths results in a series of three interacting molecules which repeats along a chain approximately developing in the *ab* plane (Figure 1, right).

A final important point to be considered is that, since the ionic radii of Co^{II} and Zn^{II} are very close to each other (0.745 vs 0.74 Å), and **1** is isomorphous with the Zn derivative, the Zn host can be considered to be isostructural with **1** in its hs-Co^{II}−SQ charge distribution, whose structure could not be solved. On its turn, this strongly suggests that the doping of Co^{II} in **1** occurs with no relevant structural variations of the host molecular structural parameters. This could be tested by recording the X-ray powder diffractogram of the 50% doped Zn derivative of **1** and comparing it with the theoretical diffractogram expected for the pure $[Zn(Me_2tpa)(DBSQ)](PF_6) \cdot C_6H_5CH_3$ (Figure SI1, Supporting Information). All the peaks in the theoretical diffractogram are observed in the doped compound indicating that upon doping the crystal structure is maintained. Furthermore, since no extra peaks are observed, it can be safely concluded that only one, homogeneous, crystalline form is present in the sample, confirming the formation of mixed Zn/Co crystals.

Magnetic Properties: Entropy Driven VT. The temperature dependence of the valence tautomeric equilibrium for the four solid solutions of **1** in the homologous Zn-based host has been followed by magnetometric means and is reported in Figure 2a as hs-Co^{II} −SQ molar fraction vs T. This value has been extracted from the measured data, which include the contribution of the host lattice, using the simple relation:

$$\chi_M T_{CoSQ} = \frac{\chi_M T_{meas} - (1-x)\chi_M T_{ZnSQ}}{x} \qquad (1)$$

where x is the molar ratio of **1** into the doped crystalline environment and $\chi_M T_{CoSQ}$, $\chi_M T_{meas}$ and $\chi_M T_{ZnSQ}$ are the products of the molar magnetic susceptibility of **1**, of the doped system and of the Zn host times the temperature.

These data show that the entropy driven transition becomes more gradual on increasing dilution. This behavior is well documented for solid solutions of spin crossover complexes,[48,49,59] and it has been usually assigned to the loss of cooperativity of the interconverting centers, since this interaction can be assumed to be proportional to the square of the molar fraction of the interacting species, $\gamma_{Co^{II}-SQ}^2$.[60] Furthermore, the analysis of T_c for the different solid solutions (Figure 2b) evidences that the thermal interconversion temperature, T_c, shifts toward low temperature with an increasing dilution. The observed pattern can be explained in terms of change of internal pressure, determined by the radius of the ions of the host. Indeed, when the host is made up of ions with larger radii than the guest one, it can be considered to exert a "negative pressure" on the guest system, thus, favoring the interconversion toward the largest species. The effect of a smaller ionic radius for the host compared

(58) Pierpont, C. G.; Buchanan, R. M. *Coord. Chem. Rev.* **1981**, *38*, 45–87.
(59) Martin, J.-P.; Zarembowitch, J.; Bousseksou, A.; Dworkin, A.; Haasnoot, J. G.; Varret, F. *Inorg. Chem.* **1994**, *33*, 6325–6333.
(60) Spiering, H. *Top. Curr. Chem.* **2004**, *235*, 171–195.

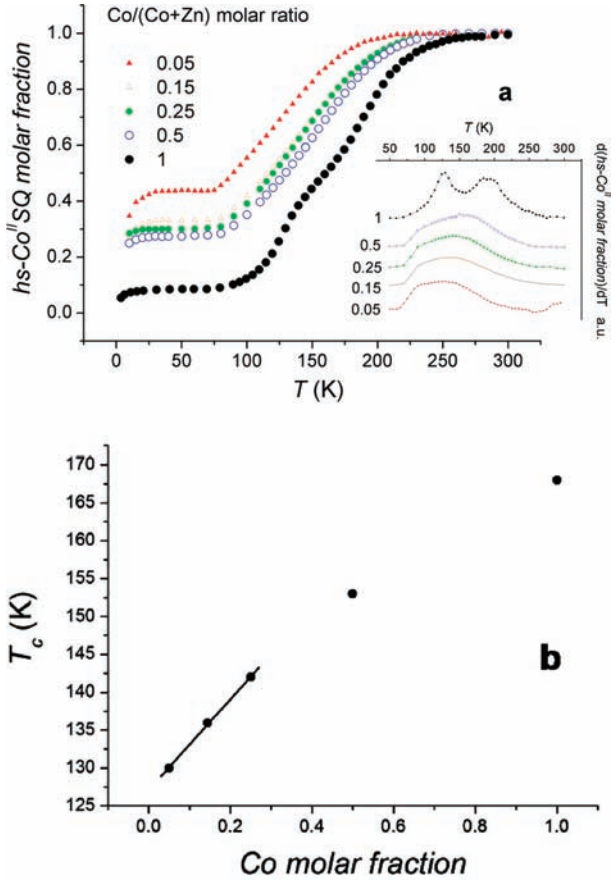

Figure 2. (a) Thermal evolution of the hs-Co^{II} molar fraction with temperature for a series of differently diluted solid solutions of **1**. The inset is evidence the transition temperature obtained by plotting the temperature dependence of the derivative of the hs-Co^{II} molar fraction with respect to T. (b) T_c dependence of the solid solutions of **1** on the Co/(Co + Zn) molar ratio. The black line is the best linear fit obtained at low-Co concentration.

to the guest is the opposite. Since the ionic radius of the Zn^{II} ion is very similar to that of the hs-Co^{II} ion and is much larger than the ls-Co^{III} one (0.545 Å), the induced negative pressure stabilizes the Co^{II}−semiquinonato species, leading to a decrease of T_c with increasing dilution. At low Co molar fractions, we found an approximately linear dependence of T_c on the Co concentration in the sample, with a rate of T_c variation of 69(2) K/Co molar fraction in the solid solution and an estimated conversion temperature at infinite dilution of 126.6(6) K. Finally, an enhancement of the residual Co^{II}−semiquinonato species is observed with increasing dilution. Again this can be explained by taking into account the negative pressure of the host lattice. All of the observed data compare well with those of the similar ones reported for spin crossover complexes.[48,49,59] For these systems, both enthalpy and entropy changes associated with the spin conversion decrease with dilution, if a negative pressure is operative. In particular, the determining role of vibrational entropy change with dilution has been recently stressed by Real and co-workers.[61]

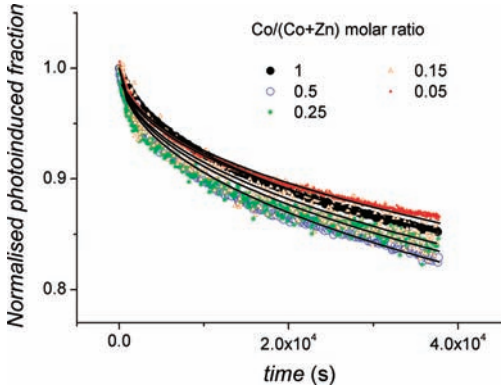

Figure 3. Normalized converted fraction $\gamma(t)$ decay after laser irradiation at 904 nm at 9 K for differently diluted solid solutions of **1** in its zinc analogue. The full lines are the fitting curves whose equations are described in the text.

Magnetic Properties: Optically Driven VT. We went further, investigating the dynamics of relaxation of the photoinduced metastable state in the function of solid dilution. Following the same procedure previously reported for **1**, the four solid solutions were irradiated at 904 nm and 9 K to induce the interconversion of Co^{III}−catecholato to Co^{II}−semiquinonato moieties. The decay of the photoinduced metastable state to the ground state has been measured at the same temperature by recording the time-dependent magnetization of the samples 35 s after having switched off the light source at the photostationary limit of each sample, in order to get insight into the low-temperature tunneling relaxation regime of **1**. The normalized converted paramagnetic molar fraction γ vs time patterns are shown in Figure 3.

The relaxation times at 9 K, obtained for the pure compound as well as its four solutions, are almost independent of the degree of metal dilution. This has been confirmed by fitting each curve using a phenomenological approach for the analysis of dynamics of bistable systems, first employed for the investigation of magnetic relaxation in field-cooled spin glasses[63] and later used for characterizing the relaxation decay of valence tautomeric compounds.[28−30,52,53,63,64] The relation, shown as eq 2, describes deviations from a monoexponential behavior of the isothermal decay of the photoinduced metastable state:

$$\gamma(t) = \gamma(0)e^{-\left(\frac{t}{\tau}\right)^{\beta}} \qquad (2)$$

In eq 2, $\gamma(0)$ is the photoinduced hs-Co^{II}SQ molar fraction at the beginning of the decay, τ is the relaxation time (the time required for $\gamma(t)$ to be reduced at $\gamma(0)/e$ its value), and β is a phenomenological parameter taking into account the deviation from single-exponential relaxation behavior ($\beta = 1$, single relaxation mechanism, and $\beta \neq 1$ distribution of relaxation rates).[63] The relaxation times obtained fitting the time evolution of the hs-Co^{II}SQ molar fraction shown in Figure 3 with eq 2 are: $\tau(1.00) = (1.481 \pm 0.004) \times 10^6$ s; $\tau(0.50) = (1.021 \pm 0.003) \times 10^6$ s; $\tau(0.25) = (1.158 \pm 0.008) \times 10^6$ s; $\tau(0.15) = (1.264 \pm 0.011) \times 10^6$ s; and $\tau(0.05) = (1.665 \pm 0.004) \times 10^6$ s.

(61) Tayagaki, T.; Galet, A.; Molnàr, G.; Carmen Munoz, M.; Zwick, A.; Tanaka, K.; Real, J.-A.; Bousseksou, A. *J. Phys. Chem. B* **2005**, *109*, 14859–14867.
(62) Chamberlin, R. V.; Mozurkewich, G.; Orbach, R. *Phys. Rev. Lett.* **1984**, *52*, 867–870.
(63) Carbonera, C.; Dei, A.; Létard, J.-F.; Sangregorio, C.; Sorace, L. *Inorg. Chim. Acta* **2007**, *360*, 3825–3828.
(64) Cui, A.; Takahashi, K.; Fujishima, A.; Sato, O. *J. Photochem. Photobiol., A* **2004**, *167*, 69–73.

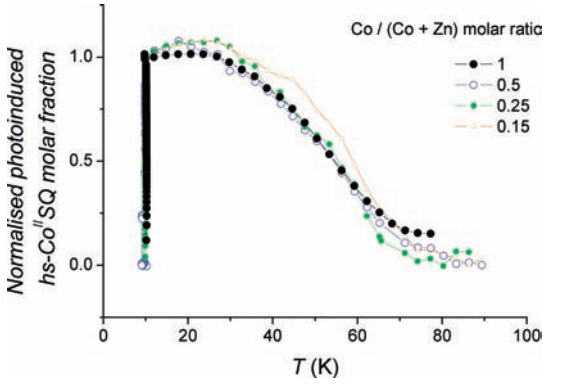

Figure 4. T_{LIESST} pattern for **1** and its solid solutions at different dilution percentages.

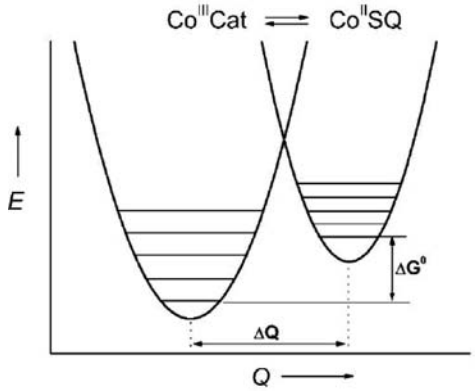

Figure 5. Double well potential scheme of the energy levels involved into the valence tautomeric interconversion at low temperature in Co−dioxolene systems.

In order to reduce the correlation between the τ and β parameters, the β parameter was kept fixed at a value of 0.5. These results fully agree with a decay process independent of the concentration of the metastable species.

Finally, the relaxation features of **1** in the thermally assisted relaxation regimes have been characterized measuring the T_{LIESST} values of the different solid solutions. The results are shown in Figure 4, reporting the temperature dependence of the normalized photoinduced hs-Co^{II}SQ molar fraction.

It is rather evident that the T_{LIESST} values for the solid solutions at different Co concentrations are, in practice, the same within our experimental error.

Discussion

The relaxation of the photoinduced metastable state to the thermodynamic stable one involves an intersystem crossing process (ISC) because of the different spin multiplicity of the two redox isomers. Furthermore, as already mentioned in the introduction, the interconversion process involves large changes in bond lengths between the acceptor and the donor atoms. For the sake of simplicity, we focus our attention on Co−O bond lengths. The difference of about 0.2 Å observed at high temperatures for the two redox isomers[52,53] is maintained at cryogenic temperatures, as supported by EXAFS experiments.[65] In analogy with spin crossover complexes, the relaxation decay of the optically induced metastable species can be treated as a nonadiabatic process within the framework of the Jortner radiationless multiphonon relaxation.[50,66] The treatment is expected to work in the limit of strong vibronic coupling between two different spin states in different nuclear configurations and clearly predicts a thermally activated behavior of the relaxation decay as well as a temperature-independent relaxation rate at cryogenic temperatures. The latter phenomenon is explained in terms of the tunnel effect between the vibronic levels belonging to different electronic states. In a simplified view, the phenomenon is usually described by means of the energy potential diagram where the two redox isomers Co^{III}−Cat and Co^{II}−SQ are represented by the two harmonic potential energy curves.

In the present case, the Co^{III}−Cat redox isomer lies at a lower energy than Co^{II}−SQ and, therefore, constitutes the ground-state species. The reaction coordinate Q can be assumed to correspond to the total symmetric breathing mode of the complex, since the interconversion involves a change of the Co−O bond length. In classic kinetics, the relaxation rate from one state to the other is controlled by the thermal energy necessary to overcome the free energy barrier between the two potential curves. In a quantum mechanic approach, the tunneling probability for a nonradiative process is determined by both intramolecular and intermolecular vibrations. Since the latter is significantly smaller than the former, it is usually assumed that they could be simply expressed by an appropriate parameter. As a matter of fact, we have found for several 1:1 Co−dioxolene systems that the temperature dependence of the tunneling rate in the low-temperature region follows a thermally activated pseudo-Arrhenius behavior with a activation energy of 5−15 cm^{-1}, which is attributed to a process promoted by low-energy phonons.[29,30,52,53] This supports the hypothesis that the intermolecular vibrations do not play a significant role though, in principle, they cannot be neglected, since the phonon bath provides the continuum of states required for the nonadiabatic process. However, when the relaxation decay follows a thermally activated behavior, the observed activation energies lie close to 300 cm^{-1}, i.e., the value associated to the Co−O symmetric breathing mode. Therefore, in practice, the nonradiative process is determined by the overlap of a given vibrational level k of the symmetric breathing mode of the Co^{II}−SQ state and a vibrational level $i + n$ of the analogous mode of Co^{III}−Cat one. If this simplification holds, then the relaxation decay may be assumed to follow the Fermi golden rule.[41,42,67] Following this treatment, the relaxation from the metastable state is expected to slow down as the difference in bond lengths (represented in Figure 5 as ΔQ) between the two isomers increases and as the electronic coupling and the zero point energy difference (labeled ΔG^0 in Figure 5) decrease.

The obtained relaxation times for the solid solutions of **1** are related to the temperature-independent relaxation regime. Since the electronic coupling and the difference in bond lengths can be reasonably expected not to vary with

(65) Poneti, G.; Mannini, M.; Dei, A.; Sorace, L.; Sainctavit, Ph. *ESRF report*; http://ftp.esrf.eu/pub/UserReports/41417_B.pdf

(66) Buhks, E; Navon, G.; Bixon, M.; Jortner, J. *J. Am. Chem. Soc.* **1980**, *102*, 2918–2923.

(67) Gentili, P. L.; Bussotti, L.; Righini, R.; Beni, A.; Bogani, L.; Dei, A. *Chem. Phys.* **2005**, *314*, 9–17.

dilution, the above-mentioned theoretical expectations that the lifetimes of the metastable species would increase with dilution were based on the expectation of a decrease of the reduced energy gap ΔG^0, as a result of the stabilization of the metastable $Co^{II}-SQ$ species by the Zn host. The similarities of the observed lifetimes suggest that the reduced energy gap does not significantly vary upon dilution. On the other hand, the clear decrease of the critical temperature for the entropy driven transition on decreasing the Co:Zn ratio can be attributed to the negative pressure exerted by the host lattice.[48,49,59] Thus, as far as this chemical approach is used to test the cooperativity effects onto the kinetics of relaxation in tunneling conditions, we can state that optical bistability in this class of compounds is related to single-molecular properties and not to a three-dimensional network of interactions able to stabilize the photoinduced metastable state.

In this framework, also the observed independence of T_{LIESST} value from the doping level can be easily explained. Indeed, T_{LIESST} is intrinsically associated to a temperature range where the rate of decay of the metastable state is temperature dependent. Therefore, since the energies of the involved vibrational levels do not appear to vary with the dilution, it is expected that the relaxation kinetics should be characterized by similar Franck−Condon factors. If this consideration holds, then it is highly reasonable to observe similar T_{LIESST} for solid solutions at different concentrations, whereas it would be weird to obtain a different result.

Conclusions

The present contribution addresses the role of cooperativity in the solid state to the entropy and the light-driven valence tautomeric interconversion in a 1:1 Co−dioxolene complex. The approach used relies on the chemical tuning of the intermolecular interactions by the solid dissolution of **1** into the isomorphous inert crystalline lattice of its Zn-based analogue complex. The latter is expected to act a negative pressure on the lattice, stabilizing in energy the hs-$Co^{II}-SQ$ isomer, characterized by a higher molecular volume with respect to the low-temperature phase ls-$Co^{III}-Cat$. The thermal induced VT confirms its entropy driven character and features the expected overall stabilization of the hs-$Co^{II}-SQ$ isomer, increasing the degree of dilution of **1** into the inert lattice. The increase of the relaxation times with the degree of solid dilution, awaited on the basis of the inverse energy gap law currently used for the interpretation of the kinetics of decay of the photoinduced state at low temperatures in molecular bistable materials,[42] has, however, not been observed in neither the tunneling nor the classic, thermally assisted, relaxation regimes. This behavior has been attributed to the low degree of stabilization of the vibrational states of the isomers due to the dilution, since lattice phonons seem unable to improve the mixing of the vibrational functions belonging to the potential wells of the different electronic states of **1**. This was, in part, predicted by Jortner in his original work. This result is of particular interest in the bistable molecular materials' scientific community, pointing out the single-molecular character of the optically induced bistability in valence tautomeric complexes. In addition, the absence of cooperativity in the slow relaxation process of the photoinduced metastable state at low temperatures paves the way for their characterization in nanostructured environments.

Acknowledgment. We acknowledge the financial support of the EU through MOLSPINQIP (STREP 211284) and of the Italian MiUR through PRIN 2008 is gratefully acknowledged.

Supporting Information Available: Crystallographic information file (CIF) for $[Zn(Me_2tpa)(DBSQ)]PF_6 \cdot C_6H_5CH_3$ and comparison of the room-temperature X-ray powder spectrum of 50% Co-doped sample with the theoretical one calculated by the CIF file of **1**. This material is available free of charge via the Internet at http://pubs.acs.org.